IEEE Access
Multidisciplinary | Rapid Review | Open Access Journal

Received March 7, 2021, accepted March 29, 2021, date of publication March 31, 2021, date of current version April 12, 2021.

Digital Object Identifier 10.1109/ACCESS.2021.3070195

Fixed Frequency Beam-Scanning HMSIW-Based Leaky-Wave Antenna Composed of Circular Slots in V-Shape Configuration

NIMA JAVANBAKHT[1], (Member, IEEE), RONY E. AMAYA[1], (Senior Member, IEEE), JAFAR SHAKER[2], (Senior Member, IEEE), AND BARRY SYRETT[1], (Member, IEEE)

[1]Department of Electronics, Carleton University, Ottawa, ON K1S 5B6, Canada
[2]Communication Research Center, Ottawa, ON K2K 2Y7, Canada

Corresponding author: Nima Javanbakht (nima.javanbakht@carleton.ca)

This work was supported in part by the Natural Science and Engineering Research Council of Canada (NSERC).

ABSTRACT A new reconfigurable slotted antenna is presented in this manuscript. The proposed antenna is realized on a half-mode substrate integrated waveguide (HMSIW). The beam-steering is achieved using embedded varactor diodes in circular cells. Sweeping the bias voltage causes variations of the phase constant, which leads to the fixed frequency beam-scanning. Each reconfigurable cell includes a circular slot at the top plate and varactor switch, DC block, and RF block at the backside of the structure. The operating frequency is chosen as 28.5 GHz in the support of the upcoming 5G mm-wave communications systems. The proposed antenna beam scans 29° of space by switching among different states at 28.5 GHz. The length, width, and height of the antenna are 67 mm, 48 mm, and 0.32 mm, respectively. The proposed antenna's main novelties are compactness and electronic beam-scanning capability using a single switch per cell. The measured peak realized gain and sidelobe level (SLL) at 28.5 GHz are 8.2 ± 0.6 dBi and 5 dB, respectively. While the impedance bandwidth of the proposed antenna is 1.5 GHz. A good agreement between measured and simulated results is observed. The discrepancies are investigated through a sensitivity analysis. Fixed frequency beam-scanning capability, compactness, simplicity of the assembly, backward radiation, and slight gain variation of the proposed antenna make it a suitable candidate for blind-spot monitoring and 5G vehicle to everything (V2X) communications.

INDEX TERMS Antenna, beam-scanning, compact, leaky-wave, varactor diode.

I. INTRODUCTION

Antennas are critical parts of communications systems. Hence, they need to be designed to operate optimally in the face of variable operational and environmental conditions. Achieving a low-profile, low loss, medium gain, and a beam-scanning antenna is crucial to overcome the path loss and mitigate the negative impact of a dynamic propagation environment. 5G technology is a promising standard for wireless communications [1]–[8]. Deployment in a dense environment demands dynamic coverage. Hence using a fixed frequency beam-scanning antenna in 5G communication networks is beneficial.

The associate editor coordinating the review of this manuscript and approving it for publication was Diego Masotti.

Reconfigurable antenna scans space electronically [9]–[37], which is a more practical method compared to the frequency beam-scanning [38]–[56]. Furthermore, implementing a reconfigurable antenna can compensate for the unwanted beam-squint due to the variable operational and environmental conditions. Electronic beam-scanning is achieved using semiconductor switches, MEMs, or PiN diodes. GaAs varactor diodes were selected to function as switches in the proposed structure because of their small footprint, high switching speed, and robustness.

A leaky-wave antenna (LWA) is a traveling wave antenna in which the wave leaks into space through the discontinuities in the structure [9]–[32], [38]–[56]. LWAs are suitable candidates for the 5G networks due to their compactness and beam-steering capability. To achieve a compact structure, novel designs can be

realized based on a half-mode substrate integrated waveguide (HMSIW) [47]–[50], [57]–[59]. HMSIW is a compact microstrip structure in which half of the structure was removed. Furthermore, the side via fence of HMSIW confines the electromagnetic field and acts as a waveguide sidewall [57]–[59]. Noting the low profile, low cost, ease of fabrication, and beam-scanning capability of HMSIW LWA [9]–[16], it is a suitable candidate for 5G applications such as the internet of things (IoT) and vehicle to everything (V2X) communications [1], [2]. The authors first exploited the proposed idea in [15]. However, in this manuscript, electronic components were located at the back of the antenna to minimize their undesired effects on the radiation pattern due to their footprint. A detailed analysis of the experimental validations is also carried out in this paper. The key novelties of the proposed antenna can be categorized as the following: slight gain variation, operation in the mm-wave frequency band, compactness, backward beam-scanning with adequate scanning range, ease of fabrication, and low cost. These features make the proposed antenna a suitable candidate for 5G blind-spot monitoring and V2X communications.

The organization of this paper is as follows; the design method is explained in section II. The structure of the antenna is presented in section III. Measurements and the simulated results are investigated in section IV.

II. DESIGN METHOD

The primary conditions for radiating in LWA is

$$-k0 < \beta < k0 \tag{1}$$

where β and k_0 are the phase constant and free-space wavenumber, respectively [40], [41]. The proposed antenna is an electronic beam-scanning LWA based on HMSIW. The dispersion diagram of the proposed antenna for one switching state was obtained through full-wave simulations along with physical intuition, as presented in Fig. 1. According to Fig. 1, β satisfies (1) that confirms the antenna's leaky-wave nature. Moreover, the main-lobe is pointed toward backward due to the negative value of β. This indicates that our proposed LWA is suitable for backward beam-scanning.

The proposed antenna is a reconfigurable LWA based on HMSIW, as shown in Figs. 2 and 3. In LWA, β is related to the main-lobe pointing angle (θ_0) by [40], [41]

$$\cos(\theta_0) = \frac{\beta}{k_0} \tag{2}$$

S-parameters of a single cell of the structure and β are related by

$$\cosh((\alpha + j\beta)L) = \frac{S_{12}S_{21} + (1 + S_{11})(1 - S_{22})}{2S_{21}} \tag{3}$$

where α and L are the attenuation constant and length of the cell, respectively [60]. According to (2) and (3), changing the cell impedance leads to the variation of S-parameters, β, and θ_0. In other words, switching leads to beam-scanning at a fixed frequency. It should be noted that (3) only provides a general guideline on the beam-scanning mechanism since the proposed antenna is a quasi-periodic structure.

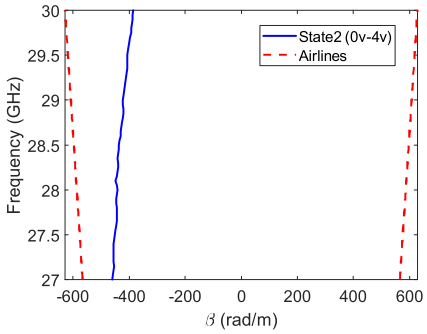

FIGURE 1. Dispersion diagram of the proposed reconfigurable HMSIW LWA.

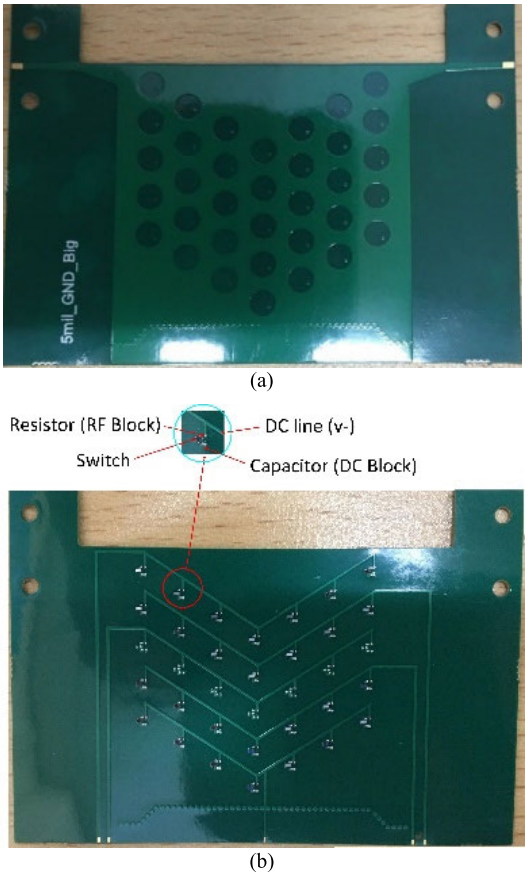

FIGURE 2. Fabricated electronic beam-scanning LWA. (a) Top view, (b) Bottom view.

The total length of the antenna depends on the size of the radiation and the feed sections. The feed length is adjusted to optimize the return loss of the antenna, while the radiation length is calculated by

$$\Delta\theta = \frac{\lambda_0}{L_r \sin\theta_0} \tag{4}$$

where $\Delta\theta$, L_r, and λ_0 are half-power beamwidth, radiation length, and free space wavelength, respectively [40], [41]. The θ_0 and $\Delta\theta$ at the center frequency (i.e., 28.5 GHz) were

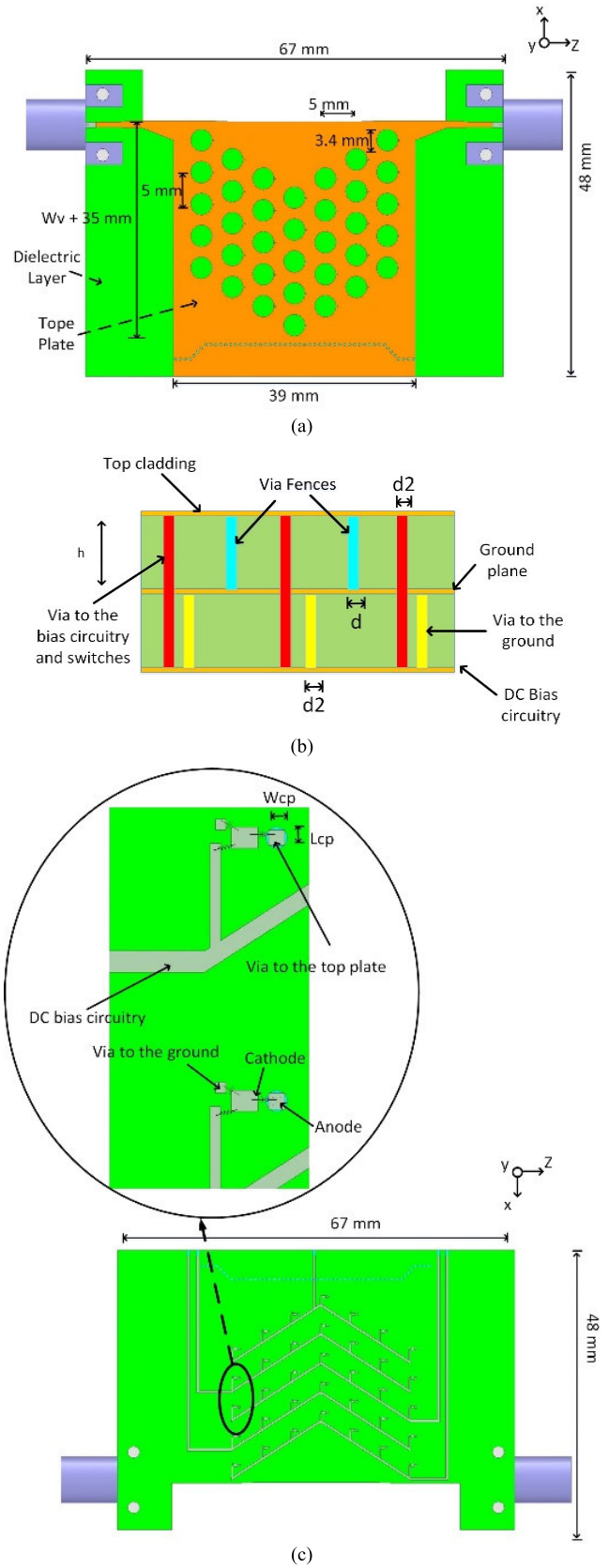

FIGURE 3. Schematic of the proposed reconfigurable leaky-wave antenna. (a) Top view, (b) Side view (not scaled), (c) Bottom view.

TABLE 1. Important geometrical parameters of the proposed reconfigurable HMSIW-based antenna.

Parameter	h	d	d_2	W_v	L_{pc}	W_{pc}
Value (mm)	0.127	0.4	0.2	0	0.3	0.3

chosen as 130° and 20°, respectively that led to $L_r = 39$ mm ($3.7\lambda_0$). It should be noticed that forward and backward end-fire directions are at $\theta = 0°$ and 180°, respectively. Therefore, θ_0 was chosen as 130° to achieve backward radiation. Due to the antenna's beam-scanning nature, $\Delta\theta$ and θ_0 change by sweeping the bias voltage or the frequency.

III. STRUCTURE OF THE ANTENNA

The proposed reconfigurable antenna was implemented on a four-layer Rogers RT/Duroid 5880 substrate with relative permittivity of 2.2, loss tangent of 0.0009, and 0.5 Oz copper cladding. This substrate was selected due to its low dielectric loss and relative permittivity to reduce the loss and the frequency beam-squint. The length, width, and height of the antenna are 67 mm, 48 mm, and 0.32 mm, respectively. The fabricated HMSIW LWA and schematic of the optimized antenna are presented in Figs. 2 and 3, respectively. It should be noted that the proposed structure contains four copper claddings, where the second and the third copper claddings were connected to create the ground plane, as shown in Fig. 3(b).

A tapered via fence in addition to tapered microstrip transition was implemented to minimize the return loss. Each end of the structure was terminated to a k-connector while one of them was terminated to a 50Ω-matched load to absorb the residual non-radiated power since at least 10% of input power in LWA remains in the guided structure [40], [41]. Placing the cells in a V-shape configuration improves the impedance matching as well. Some of the important geometrical parameters are listed in Table 1.

The proposed antenna contains thirty-five circular cells in a V-shape configuration. Each reconfigurable cell is in the shape of a circle with a diameter of 3.4 mm. The minimum size of the reconfigurable cell was dictated by the fabrication design rules, which required specific line width and spacing between components to accommodate the practical implementation. The circular shape cell leads to a more unfirm surface current distribution than the rectangular slot due to removing the sharp corners of the latter. It should be noticed that in the proposed LWA, radiation occurs from the side aperture and circular slots. The locations, the number, and the spacing of the reconfigurable cells were determined through full-wave simulation in conjunction with physical intuition to achieve the optimum beam-scanning range along with small gain variation and proper return loss. These parameters dictated the width of the HMSIW in order to achieve a desired beam-scanning range along with the adequate gain and SLL, while keeping the antenna

compact, five V-shape rows contain thirty-five cells were implemented. This resulted in a 35 mm width. The electric field distributions of HMSIW with and without slots and components are presented in Fig. 4. Because of the large width of HMSIW and feeding through surface-mounted connectors and microstrip transitions, the field distribution is different than the fundamental mode and higher-order waveguide mode is excited, as shown in Fig. 4(a). The presence of multiple nodes in the field distribution confirms the excitation of the higher-order mode. Whereas in a narrow HMSIW supporting only the fundamental mode, the maximums of the E-field are solely at the open side aperture [48]. The circular cells are placed at the locations of the maximum electric field to perturb the field and change the modal configuration more effectively, as shown in Fig. 4(b). By implementing a V-shape configuration, transverse and longitudinal components of β and the surface currents are disturbed by switching, leading to a relatively wide beam-scanning range.

The GaAs varactor diode MAVR-011020-14110P was used as the switch. According to the diode datasheet [61], sweeping the bias voltage in the range of 1-20V leads to capacitance variations of 0.15−0.035pF at room temperature. The Q factor of the MAVR-011020-14110P varactor diode is 3000 at 4V and 50 MHz [61]. A GRM0335C1H4R7CA01D chip capacitor and ERA-1AEB102C chip resistor were used as DC and RF blocks in each cell, respectively. The anode is connected to the top plate through a via, while the cathode is terminated to the bias circuitry through the RF block. To keep the structure compact, the bias circuitry is placed underneath the antenna's ground plane, as shown in Figs. 2 and 3. The RF components are placed at the backside of the antenna to minimize their footprints' effect on the radiated field. Moreover, the coupling between RF components and the top cladding is reduced by placing them at the backside. Shrinking the reconfigurable cell size results in a more compact structure. However, doing so increases the mutual coupling among the cells. The minimum cell size and period are also dictated by the fabrication technology limitations. The varactor diodes, DC blocks, and RF blocks were assembled on the pads using the ball grid array (BGA) method to minimize the inductance and resistance due to the assembly process. DC pads are connected to the DC source through sets of thin, flexible, and strong wires.

IV. SIMULATED AND MEASURED RESULTS

The full-wave simulation results were obtained using ANSYS HFSS v19.2. The center operating frequency was chosen as 28.5 GHz. S-parameters were measured using a Rohde & Schwarz ZVA-67 VNA. The gain radiation patterns were measured at an anechoic chamber. The MI-12A-26 standard gain horn antenna with the average peak gain of 23.6 dBi over the frequency bands of 27−30 GHz was used as the reference gain antenna. The measurement setups are shown in Figs. 5 and 6.

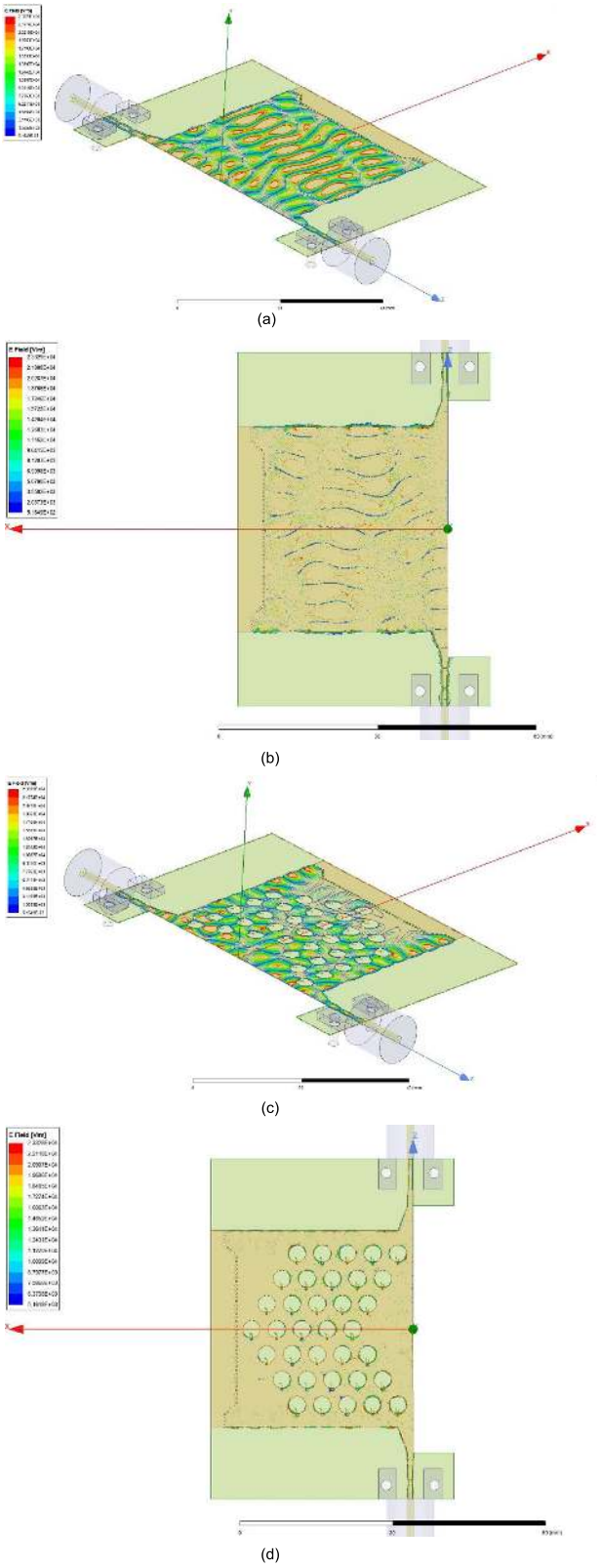

FIGURE 4. Electric field distribution. (a) 3D view of the HMSIW without slots and components, (b) Top view of the HMSIW without slots and components, (c) 3D view of the HMSIW with circular slots and components in V-shape configurations, (d) Top view of the HMSIW with circular slots and components in V-shape configurations.

FIGURE 5. S-parameters measurement setup.

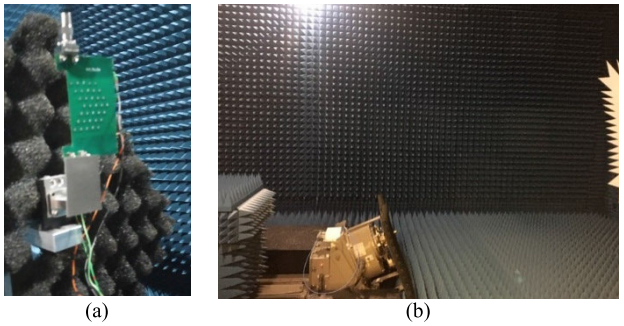

FIGURE 6. Gain radiation pattern measurement setup. (a) AUT, (b) Anechoic chamber.

Sweeping the varactor diodes bias voltage results in the variation of the series capacitance of the structure, which changes the series resonance frequency and the input impedance. This leads to variations of β and θ_0. All switches in a V-shape row were biased similarly to simplify the bias circuitry. Four switching states are reported as follows to validate the fixed frequency beam-scanning capability; (1) all switches are biased at 0V (i.e., open circuit), (2) the first two rows (i.e., closest ones to the open side aperture) are biased at 4V and the rests are biased at 0V, (3) the first two rows are biased at 15V and the rests are at 0V, and (4) all rows are biased at 1V. Unfortunately, due to the error in the antenna's fabrication, few switches in the last V-shape row (i.e., closest to the via fence) were short-circuited. Hence, the last row was not connected to the DC voltage to protect the power source. This results in deviations from the predicted and initial simulated results. It should be noted that in the presented simulated results, we considered the last row to be defective in order to capture the actual physical condition.

The measured and simulated S-parameters for different switching states are presented in Fig. 7, exhibiting return loss better than 10 dB over the frequency range from 28 to 29.5 GHz in all switching states. Since the implemented varactor diodes have constant return loss [60], there is little or no variation in the return loss (S_{11}) by sweeping the bias voltage. This is beneficial since the impedance matching is not changing severely by switching. The measured insertion loss ranges from 12 to 20 dB for different switching states over the frequency band of 27−30 GHz, which is due to the

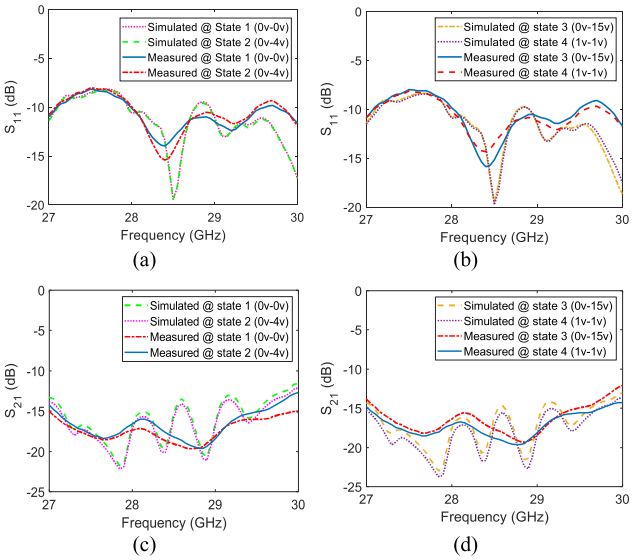

FIGURE 7. S-parameters of the proposed reconfigurable antenna at different switching states. (a) Return loss at states 1 and 2, (b) Return loss at states 3 and 4, (c) Insertion loss at states 1 and 2, and (d) Insertion loss at states 3 and 4.

radiation from slots, feed transition loss, and losses of the varactor diodes and resistors (i.e., RF blocks). The proposed LWA was realized on a thin substrate to achieve a compact structure. This resulted in a high conducting loss, low gain, and high insertion loss as well. The discrepancies between simulated and measured results will be investigated through a complete sensitivity analysis after presenting the results.

The measured and simulated radiation patterns for four different switching states at 28, 28.5, and 29 GHz are presented in Figs. 8−10 confirming fixed frequency beam-scanning capability of the proposed LWA. It should be noted that E-plane is at $\varphi = 90°$ (i.e., YZ-plane). In contrast, the H-plane is at different θ planes because the main-lobe shifts by switching. Unfortunately, measuring the H-plane was out of our measurement system's capability since tilting the antenna under test was impossible. Hence, we only reported the E-plane (YZ-plane) radiation pattern. Fig. 9 indicates that the main-lobe of the antenna scans 29° by switching at 28.5 GHz. As observed in Figs. 8−10, the main-lobe angle is pointed toward backward (i.e., $90° < \theta < 180°$). This is due to the propagation of higher-order waveguide mode and the V-shape topology of the cells. Backward beam-scanning can be used for monitoring the blind-spot of the vehicle. One of the advantages of the selected four switching states is the almost constant sidelobe level (SLL) at a fixed frequency, as shown in Figs. 8−10. It should be noted that the reported radiation pattern is the realized gain that accounted for return and insertion losses. Hence, the discrepancies in the S-parameters lead to further deviations between the measured and simulated radiation patterns. The discrepancies between the simulated and measured results will be investigated through parametric study shortly.

Although the proposed antenna is designed for fixed frequency beam-scanning applications, the main-lobe pointing

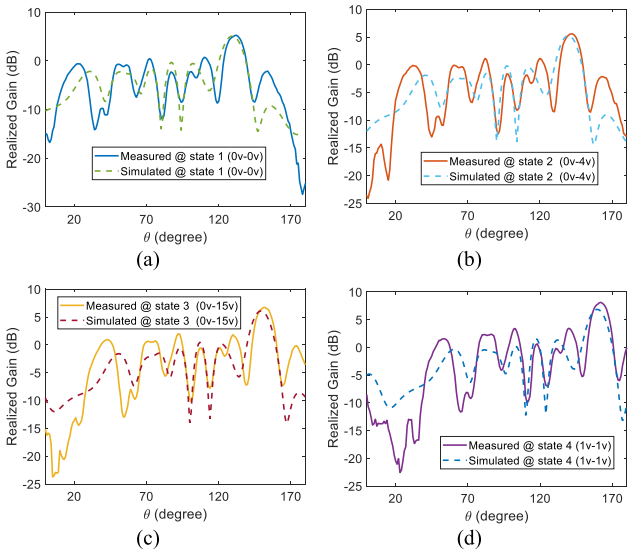

FIGURE 8. Radiation patterns of the proposed electronic beam-scanning LWA for different states in E-plane (YZ-plane) and at 28 GHz. (1) all switches are biased at 0V (i.e., open circuit), (2) the first two rows (i.e., closest ones to the open aperture) are biased at 4V and the rests are biased at 0V, (3) the first two rows are biased at 15V and the rests are biased at 0V, and (4) all rows are biased at 1V. (a) State 1, (b) State 2, (c) State 3, and (d) State 4.

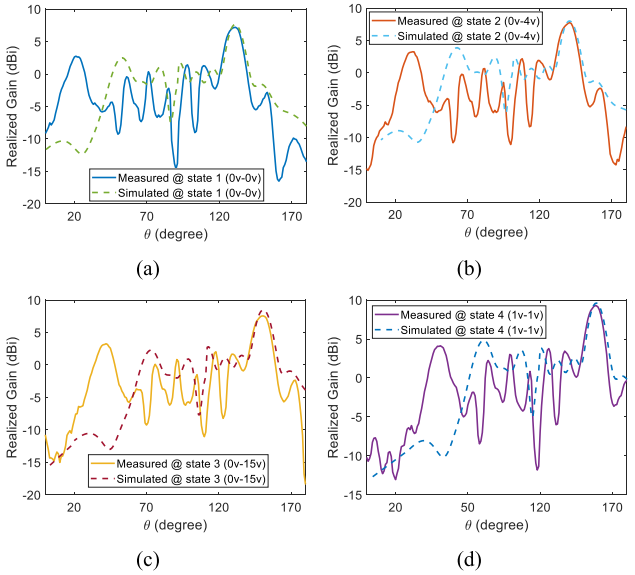

FIGURE 9. Radiation patterns of the proposed fixed frequency beam-scanning LWA for different states at 28.5 GHz. (a) State 1, (b) State 2, (c) State 3, and (d) State 4.

angel changes by sweeping the frequency due to the antenna's leaky-wave nature. The measured and the simulated frequency beam-squint in the frequency band of 27−30 GHz are 18° and 22°, respectively. As stated before, the undesired frequency beam-squint can be compensated by using the varactor diodes.

The peak realized gain for different switching states in the frequency band of 27−30 GHz are reported in Fig. 11, indicating that switching results in 1.2 dBi gain variation at 28.5 GHz. Hence, the proposed structure scans space with

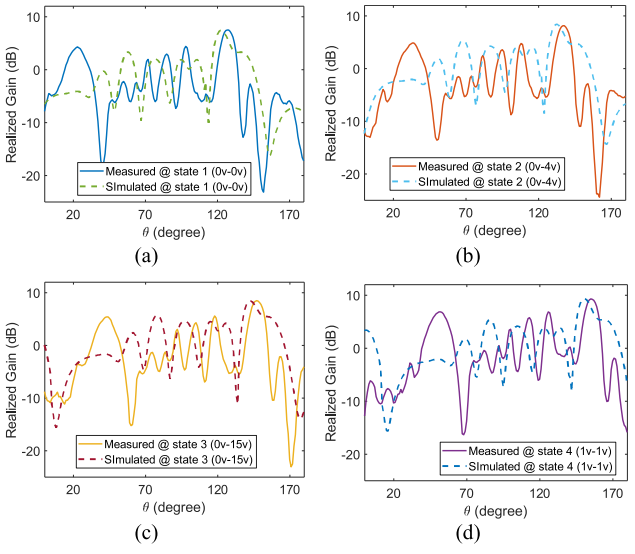

FIGURE 10. Radiation patterns of the proposed reconfigurable HMSIW LWA for different states at 29 GHz. (a) State 1, (b) State 2, (c) State 3, and (d) State 4.

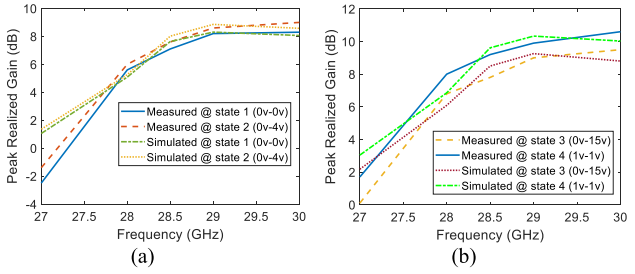

FIGURE 11. Peak realized gain of the proposed reconfigurable antenna. (a) States 1 and 2, (b) States 3 and 4.

almost constant gain at the desired frequency that is beneficial. According to Fig. 11, the measured peak realized gain varies from −2.5 to 10.6 dBi by switching over the frequency band of 27−30 GHz.

The cross-polarization radiation patterns of the proposed antenna at 28.5 GHz for four different switching states are presented in Fig. 12.

It should be noticed that the high SLL is due to the small thickness of the board and undesired reflection from the aperture [44]. Although the SLL of our proposed antenna is not optimum, it is better than the reported ones in [3], [44], and [58]. The SLL can be reduced by tapering the side via fence [46], [47] or the open side aperture [48], [49], which is the subject of ongoing research. Realizing the proposed design on a thicker substrate can improve the gain by reducing the conductor loss and improving the impedance matching. However, this is achieved at the expense of compromising the compact nature of the antenna. The gain can also be increased by increasing the number of cells at the expense of the cost and size of the antenna. Biasing the switches non-uniformly provides more switching states and results in more variations in the phase constant. Hence, achieving a wider beam-scanning range will be possible at

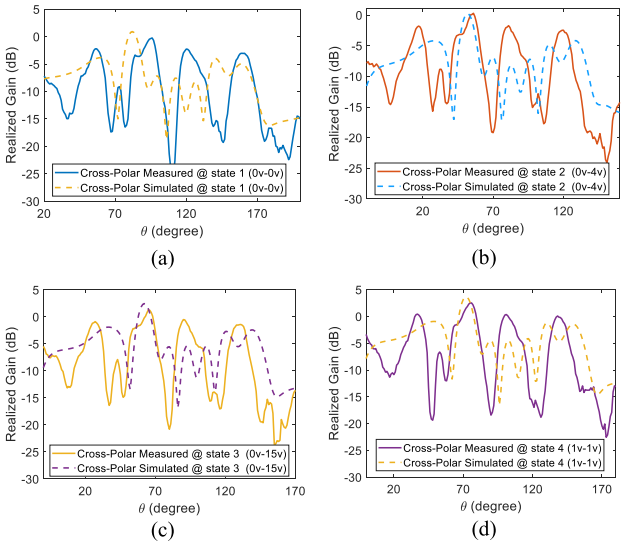

FIGURE 12. Cross-polarization radiation patterns of the proposed LWA for different switching states at 28.5 GHz. (a) State 1, (b) State 2, (c) State 3, (d) State 4.

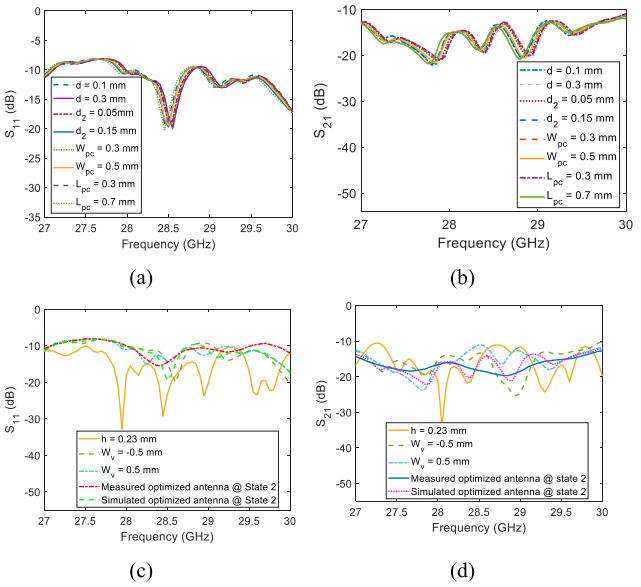

FIGURE 13. S-parameters for different geometrical parameters at state 2. (a) S_{11} for different values of d, d_2, W_{pc}, and L_{pc}, (b) S_{21} for different values of d, d_2, W_{pc}, and L_{pc}, (c) S_{11} for optimized structure along with different values of h and W_v, (d) S_{21} for optimized structure along with different values of h and W_v.

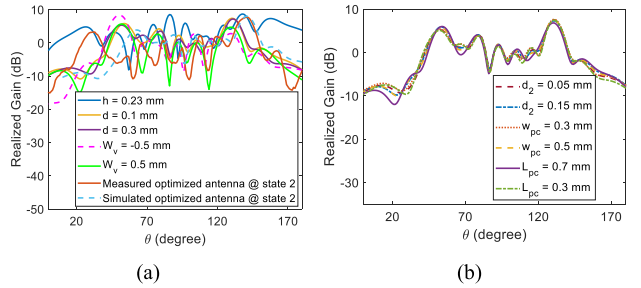

FIGURE 14. Radiation patterns at state 2 for different geometrical configurations along with the optimized structure at 28.5 GHz. (a) Different values of h, d, and W_v, (b) Different values of d_2, W_{pc}, and L_{pc}.

FIGURE 15. Schematic view of the bent reconfigurable HMSIW LWA. (a) 3D view, (b) Side view.

the expense of increasing the feed network's complexity and cost. Increasing the variable capacitance range of the switches also increases the beam-scanning range. However, achieving a high speed and low loss switch with a wide variable capacitance range at the mm-wave band is a practical challenge.

A sensitivity analysis was performed to investigate the discrepancies between simulated and measured results more thoroughly. Therefore, several parameters such as height (h), vias size (d and d_2), extension width of the waveguide section (W_v), and pad sizes (L_{pc} and W_{pc}) were changed. S-parameters and radiation patterns for different combinations are demonstrated in Figs. 13 and 14. The reported radiation pattern in Fig. 14 is at 28.5 GHz. According to the sensitivity analysis, h and W_v contribute the most to the discrepancies between measurements and simulations. In other words, the unwanted variations in h and W_v (because of the possible fabrication errors) can degrade the optimized antenna's performance, which can lead to large discrepancies between the measured and the simulated results. As reported in [44], increasing h in a conventional HMSIW, supporting the fundamental mode, leads to the SLL improvement. While this trend was not observed in our case, which can be attributed to the excitation of the higher-order mode.

The proposed antenna may bend under physical pressure because of the relatively small thickness of the substrate. Moreover, mounting the connectors may bend the ends of the antenna. This is a real concern and a possible reason for the discrepancies between the measured and the simulated results, which need to be investigated. Therefore, the antenna was gradually bent such the vertical distance from the horizon changed up to $h_b = 5.6$ mm by moving toward the two ends, as shown in Fig. 15. The S-parameters, normalized radiation patterns, and peak realized gain of the bent reconfigurable HMSIW LWA are demonstrated in Figs. 16−18 confirming the large degradations in the antenna performance in terms of return loss, peak realized gain, and radiation pattern. Overall, the possible bending of the antenna and the error in placing the via fence lead to relatively large discrepancies between the simulated and the measured S-parameters, θ_0, $\Delta\theta$, SLL, and peak realized gain.

A comparison with similar fixed frequency beam-scanning antennas in [9]–[14] is shown in Table 2. The reported operating frequency bands of [10]–[14] are lower than our proposed antenna operating in 5G mm-wave frequency band. This is one of the key differences between our proposed antenna

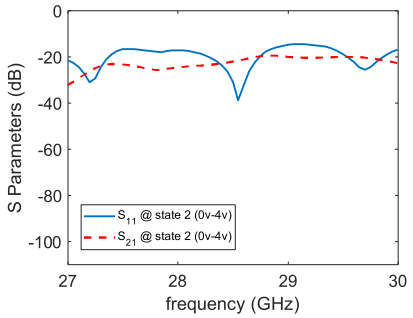

FIGURE 16. S-parameters of the bent fixed frequency beam-scanning antenna at state 2.

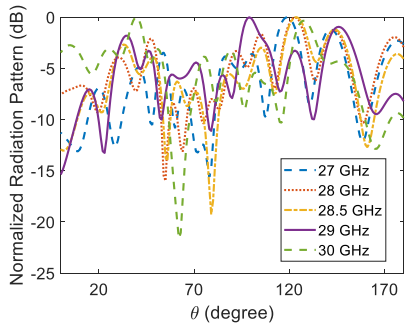

FIGURE 17. Normalized radiation patterns of the bent fixed frequency beam-scanning LWA at state 2 for different frequencies.

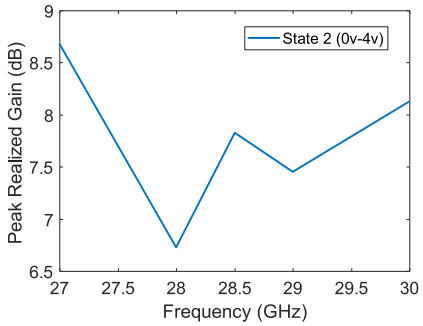

FIGURE 18. Peak realized gain of the bent reconfigurable MHSIW LWA at state 2.

and the reported ones in [10]–[14]. Considering the recent 5G developments, operating at mm-wave is an indispensable requirement for the antennas. Moreover, operating at high frequency bands leads to smaller device implementation, which is beneficial since more elements can be integrated into a given allocated area. It should be noted that by increasing the frequency, the loss and the parasitic effects of the electronic components increases. Therefore, the performance of the antennas reported in [10]–[14] may degrade if the same designs are scaled for operating at the mm-wave frequency band.

Our proposed antenna's beam-scanning range is broader than the reported ones in [9]–[11] and comparable to [12]. The wider beam-scanning range of [13] and [14] are due to the different methods that were applied to achieve the electronic beam-scanning. The reconfigurable cells of our proposed design are integrated into HMSIW, while cells are added as extra stubs to the HMSIW in [9]–[14]. Moreover, the beam-scanning in [14] was achieved using two sets of series and parallel switches, while we only use one switch per cell in our approach.

TABLE 2. Comparison among our proposed antenna and the similar reported fixed frequency beam-scanning antennas in [9]–[14].

Design	Scanning Range	Antenna Type	Peak Gain (dBi)	Center Frequency	Antenna Length
This paper	29°	HMSIW with switches at the back in V-shape	8.2 ± 0.6	28.5 GHz	3.7 λ
[9]	21°	HMSIW with tunable grounded aperture	12 ± 1.5	24 GHZ	6.7 λ
[10]	23°	HMSIW with variable capacitors	13 ± 0.84	10.8 GHZ	7.6 λ
[11]	16°	HMSIW with tunable grounded aperture	10 ± 2	6.5 GHZ	5.36 λ
[12]	29°	HMSIW with tunable grounded aperture	12.9 ± 0.6	6 GHZ	5.32 λ
[13]	39°	HMSIW with Inclined patches	10.47 ± 0.65	4.2 GHZ	3 λ
[14]	66°	HMSIW with interdigital slots	9.55 ± 1.75	6.5 GHZ	3.25 λ

The beam-scanning range should be considered in light of the gain variation. The most stringent gain variation (i.e., ±0.6 dBi) was chosen as the baseline to define the beam-scanning range in our proposed work. Overall, the gain variation of our proposed reconfigurable antenna is smaller than the ones in [9]–[11] and [14], and comparable to [12] and [13]. This is beneficial because the gain variation in the beam-scanning applications should be minimized. It should be noted that a more generous allowance of the gain variation would lead to an over-optimistic estimate of the beam-scanning range.

The radiating length of our proposed antenna is smaller than the reported ones in [9]–[12]. This is advantageous since the size is a premium in beam-scanning applications. The higher peak gain of the presented antennas in [9]–[12] are due

to the longer electric length of the reported structures. The smaller thickness of our structure leads to higher conductor loss and smaller gain than [13] and [14], which have a smaller electric length than ours. This is the price of achieving a low-profile antenna.

As stated before, the electronic components were located at the backside of our proposed antenna. This is another distinction of our work compared to [9]–[14]. This led to the ease of the fabrication and assembly because of the larger available space at the backside. Moreover, the main-beam of our proposed antenna is pointed backward, which is useful for monitoring the blind-spot in the autonomous vehicle.

Overall, small gain variations, operating in the mm-wave frequency band, compactness, ease of fabrication, and backward electronic beam-scanning make the proposed HMSIW LWA a suitable candidate for 5G V2X communications and blind-spot monitoring.

V. CONCLUSION

In this paper, a novel fixed frequency beam-scanning antenna was introduced. The proposed antenna is an HMSIW LWA with embedded electronic components. Sweeping the bias voltage of the varactor diodes changes the impedance of the cells leading to the beam-scanning. One of the key novelties of the proposed design is the integration of the reconfigurable cells at the backside of the radiating section. Therefore, the undesired effects of the footprints of the electronic components on the antenna radiation pattern were minimized. The proposed antenna scanned 29° of space with the peak realized gain of 8.2 ± 0.6 dBi at 28.5 GHz. The impedance bandwidth was 1.5 GHz. Implementing more cells and biasing them non-uniformly increase the scanning range and the gain at the expense of increasing the size, the complexity of bias circuitry, and the fabrication cost. The low-profile, backward radiation, slight gain variation, low cost of fabrication, and fixed frequency beam-scanning capability are among the features of the proposed reconfigurable LWA, which make it a suitable candidate for 5G mm-wave V2X communications, radar systems, and blind-spot monitoring.

REFERENCES

[1] J. G. Andrews, S. Buzzi, W. Choi, S. V. Hanly, A. Lozano, A. C. K. Soong, and J. C. Zhang, "What will 5G be?" *IEEE J. Sel. Areas Commun.*, vol. 32, no. 6, pp. 1065–1082, Jun. 2014.

[2] M. Shafi, A. F. Molisch, P. J. Smith, T. Haustein, P. Zhu, P. De Silva, F. Tufvesson, A Benjebbour, and G. Wunder, "5G: A tutorial overview of standards, trials, challenges, deployment, and practice," *IEEE J. Sel. Areas Commun.*, vol. 35, no. 6, pp. 1201–1220, Jun. 2017.

[3] T. Tuovinen, N. Tervo, and A. Pärssinen, "Analyzing 5G RF system performance and relation to link budget for directive MIMO," *IEEE Trans. Antennas Propag.*, vol. 65, no. 12, pp. 6636–6645, Dec. 2017.

[4] T. S. Rappaport, Y. Xing, G. R. MacCartney, A. F. Molisch, E. Mellios, and J. Zhang, "Overview of millimeter wave communications for fifth-generation (5G) wireless networks—With a focus on propagation models," *IEEE Trans. Antennas Propag.*, vol. 65, no. 12, pp. 6213–6230, Dec. 2017.

[5] N. Ojaroudiparchin, M. Shen, S. Zhang, and G. F. Pedersen, "A switchable 3-D-coverage-phased array antenna package for 5G mobile terminals," *IEEE Antennas Wireless Propag. Lett.*, vol. 15, pp. 1747–1750, 2016.

[6] W. Hong, Z. H. Jiang, C. Yu, J. Zhou, P. Chen, Z. Yu, H. Zhang, B. Yang, X. Pang, M. Jiang, Y. Cheng, M. K. T. Al-Nuaimi, Y. Zhang, J. Chen, and S. He, "Multibeam antenna technologies for 5G wireless communications," *IEEE Trans. Antennas Propag.*, vol. 65, no. 12, pp. 6231–6249, Dec. 2017.

[7] S. Zhang, I. Syrytsin, and G. F. Pedersen, "Compact beam-steerable antenna array with two passive parasitic elements for 5G mobile terminals at 28 GHz," *IEEE Trans. Antennas Propag.*, vol. 66, no. 10, pp. 5193–5203, Oct. 2018.

[8] Y. Yashchyshyn, K. Derzakowski, G. Bogdan, K. Godziszewski, D. Nyzovets, C. H. Kim, and B. Park, "28 GHz switched-beam antenna based on S-PIN diodes for 5G mobile communications," *IEEE Antennas Wireless Propag. Lett.*, vol. 17, no. 2, pp. 225–228, Feb. 2018.

[9] S. Muhammad, A. Ali, Z. Ahmed, and M. Bin Ihsan, "Beam steering in HMSIW LWA at fixed millimeter wave frequency," in *Proc. 12th Int. Conf. High-Capacity Opt. Netw. Emerg. Tech.*, 2015, pp. 91–92.

[10] M. Singh and B. Ghosh, "Periodic strip loaded reconfigurable half-mode substrate integrated waveguide-based leaky wave antennas," *Electron. Lett.*, vol. 56, no. 13, pp. 646–648, Jun. 2020.

[11] D. K. Karmokar, D. N. P. Thalakotuna, K. P. Esselle, L. Matekovits, and M. Heimlich, "Reconfigurable half-width microstrip leaky-wave antenna for fixed-frequency beam scanning," in *Proc. 7th Eur. Conf. Antennas Propag.*, 2013, pp. 1314–1317.

[12] D. K. Karmokar, K. P. Esselle, and S. G. Hay, "Fixed-frequency beam steering of microstrip leaky-wave antennas using binary switches," *IEEE Trans. Antennas Propag.*, vol. 64, no. 6, pp. 2146–2154, Jun. 2016.

[13] M. K. Mohsen, M. S. M. Isa, A. A. M. Isa, M. K. Abdulhameed, and M. L. Attiah, "Achieving fixed-frequency beam scanning with a microstrip leaky-wave antenna using double-gap capacitor technique," *IEEE Antennas Wireless Propag. Lett.*, vol. 18, no. 7, pp. 1502–1506, Jul. 2019.

[14] A. Suntives and S. V. Hum, "A fixed-frequency beam-steerable half-mode substrate integrated waveguide leaky-wave antenna," *IEEE Trans. Antennas Propag.*, vol. 60, no. 5, pp. 2540–2544, May 2012.

[15] N. Javanbakht, B. Syrett, R. E. Amaya, and J. Shaker, "Electronic beam scanning leaky-wave antenna based on delta shape half-mode substrate integrated waveguide," in *Proc. 14th Eur. Conf. Antennas Propag. (EuCAP)*, Copenhagen, Denmark, Mar. 2020, pp. 1–4.

[16] A. Suntives and S. V. Hum, "An electronically tunable half-mode substrate integrated waveguide leaky-wave antenna," in *Proc. 5th Eur. Conf. Antennas Propag.*, 2011, pp. 3670–3674.

[17] D. K. Karmokar, D. N. P. Thalakotuna, K. P. Esselle, M. Heimlich, and L. Matekovits, "Fixed-frequency beam steering from a stub-loaded microstrip leaky-wave antenna," in *Proc. Int. Symp. Electromagn. Theory*, 2013, pp. 436–439.

[18] P. Bajurko and Y. Yashchyshyn, "Design and investigation of the leaky-wave antenna with reconfigurable operating frequency," in *Proc. Eur. Conf. Antennas Propag.*, 2009, pp. 3753–3756.

[19] Y. Geng, J. Wang, Y. Li, Z. Li, M. Chen, and Z. Zhang, "Radiation pattern-reconfigurable leaky-wave antenna for fixed-frequency beam steering based on substrate-integrated waveguide," *IEEE Antennas Wireless Propag. Lett.*, vol. 18, no. 2, pp. 387–391, Feb. 2019.

[20] T. Lou, X.-X. Yang, H. Qiu, Q. Luo, and S. Gao, "Low-cost electrical beam-scanning leaky-wave antenna based on bent corrugated substrate integrated waveguide," *IEEE Antennas Wireless Propag. Lett.*, vol. 18, no. 2, pp. 353–357, Feb. 2019.

[21] K. Chen, Y. H. Zhang, S. Y. He, H. T. Chen, and G. Q. Zhu, "An electronically controlled leaky-wave antenna based on corrugated SIW structure with fixed-frequency beam scanning," *IEEE Antennas Wireless Propag. Lett.*, vol. 18, no. 3, pp. 551–555, Mar. 2019.

[22] Y. Ji, L. Ge, J. Wang, Q. Chen, and W. Wu, "Simple beam scanning SIW cavity-backed slot antenna using postloaded varactor," *IEEE Antennas Wireless Propag. Lett.*, vol. 18, no. 12, pp. 2761–2765, Dec. 2019.

[23] S. Lim, C. Caloz, and T. Itoh, "Metamaterial-based electronically controlled transmission-line structure as a novel leaky-wave antenna with tunable radiation angle and beamwidth," *IEEE Trans. Microw. Theory Techn.*, vol. 53, no. 1, pp. 161–172, Dec. 2005.

[24] S. Lim, C. Caloz, and T. Itoh, "Electronically scanned composite right/left handed microstrip leaky-wave antenna," *IEEE Microw. Wireless Compon. Lett.*, vol. 14, no. 6, pp. 277–279, Jun. 2004.

[25] S.-L. Chen, D. K. Karmokar, Z. Li, P.-Y. Qin, R. W. Ziolkowski, and Y. J. Guo, "Continuous beam scanning at a fixed frequency with a composite right-/left-handed leaky-wave antenna operating over a wide frequency band," *IEEE Trans. Antennas Propag.*, vol. 67, no. 12, pp. 7272–7284, Dec. 2019.

[26] J.-H. Fu, A. Li, W. Chen, B. Lv, Z. Wang, P. Li, and Q. Wu, "An electrically controlled CRLH-inspired circularly polarized leaky-wave antenna," *IEEE Antennas Wireless Propag. Lett.*, vol. 16, pp. 760–763, 2017.
[27] Z. Li, Y. Jay Guo, S.-L. Chen, and J. Wang, "A period-reconfigurable leaky-wave antenna with fixed-frequency and wide-angle beam scanning," *IEEE Trans. Antennas Propag.*, vol. 67, no. 6, pp. 3720–3732, Jun. 2019.
[28] L. Huang, J.-C. Chiao, and M. P. De Lisio, "An electronically switchable leaky wave antenna," *IEEE Trans. Antennas Propag.*, vol. 48, no. 11, pp. 1769–1772, Nov. 2000.
[29] B. Xi, Y. Li, Z. Liang, S. Zheng, Z. Chen, and Y. Long, "Periodic fixed-frequency staggered line leaky wave antenna with wide-range beam scanning capacity," *IEEE Access*, vol. 7, pp. 146693–146701, 2019.
[30] T. Zvolensky, D. Chicherin, A. V. Räisänen, and C. Simovski, "Leaky-wave antenna based on micro-electromechanical systems-loaded microstrip line," *IET Microw., Antennas Propag.*, vol. 5, no. 3, pp. 357–363, 2011.
[31] D. F. Sievenpiper, "Forward and backward leaky wave radiation with large effective aperture from an electronically tunable textured surface," *IEEE Trans. Antennas Propag.*, vol. 53, no. 1, pp. 236–247, Jan. 2005.
[32] R. Shaw and M. K. Mandal, "Broadside scanning fixed frequency LWA with simultaneous electronic control of beam angle and beamwidth," *IEEE Trans. Antennas Propag.*, vol. 68, no. 5, pp. 3504–3514, May 2020.
[33] A. Darvazehban, S. A. Rezaeieh, and A. M. Abbosh, "Programmable metasurface antenna for electromagnetic torso scanning," *IEEE Access*, vol. 8, pp. 166801–166812, 2020.
[34] M. A. Towfiq, I. Bahceci, S. Blanch, J. Romeu, L. Jofre, and B. A. Cetiner, "A reconfigurable antenna with beam steering and beamwidth variability for wireless communications," *IEEE Trans. Antennas Propag.*, vol. 66, no. 10, pp. 5052–5063, Oct. 2018.
[35] S. Soltani, P. Lotfi, and R. D. Murch, "Design and optimization of multiport pixel antennas," *IEEE Trans. Antennas Propag.*, vol. 66, no. 4, pp. 2049–2054, Apr. 2018.
[36] P. Lotfi, S. Soltani, and R. D. Murch, "Printed endfire beam-steerable pixel antenna," *IEEE Trans. Antennas Propag.*, vol. 65, no. 8, pp. 3913–3923, Aug. 2017.
[37] D. Rodrigo and L. Jofre, "Frequency and radiation pattern reconfigurability of a multi-size pixel antenna," *IEEE Trans. Antennas Propag.*, vol. 60, no. 5, pp. 2219–2225, May 2012.
[38] F. Monticone and A. Alu, "Leaky-wave theory, techniques, and applications: From microwaves to visible frequencies," *Proc. IEEE*, vol. 103, no. 5, pp. 793–821, May 2015.
[39] D. R. Jackson, C. Caloz, and T. Itoh, "Leaky-wave antennas," *Proc. IEEE*, vol. 100, no. 7, pp. 2194–2206, Jul. 2012.
[40] C. A. Balanis, *Modern Antenna Handbook*, 1st ed. New York, NY, USA: Wiley, 2008.
[41] J. L. Volakis, *Antenna Engineering Handbook*, 4th ed. New York, NY, USA: McGraw-Hill, 2007.
[42] F. B. Gross, *Frontiers in Antennas: Next Generation Design and Engineering*, 1st ed. New York, NY, USA: McGraw-Hill, 2011.
[43] X. Zou, C. Tong, H. He, and F. Geng, "Edge-radiating slot antenna based on half-mode substrate integrated waveguide," *IET Microw., Antennas Propag.*, vol. 11, no. 8, pp. 1106–1112, Jun. 2017.
[44] J. Xu, W. Hong, H. Tang, Z. Kuai, and K. Wu, "Half-mode substrate integrated waveguide (HMSIW) leaky-wave antenna for millimeter-wave applications," *IEEE Antennas Wireless Propag. Lett.*, vol. 7, pp. 85–88, 2008.
[45] A. Sarkar and S. Lim, "60 GHz compact larger beam scanning range PCB leaky-wave antenna using HMSIW for millimeter-wave applications," *IEEE Trans. Antennas Propag.*, vol. 68, no. 8, pp. 5816–5826, Aug. 2020.
[46] N. Nguyen-Trong, L. Hall, and C. Fumeaux, "Transmission-line model of nonuniform leaky-wave antennas," *IEEE Trans. Antennas Propag.*, vol. 64, no. 3, pp. 883–893, Mar. 2016.
[47] N. Nguyen-Trong, T. Kaufmann, and C. Fumeaux, "A wideband omnidirectional horizontally polarized traveling-wave antenna based on half-mode substrate integrated waveguide," *IEEE Antennas Wireless Propag. Lett.*, vol. 12, pp. 682–685, 2013.
[48] N. Javanbakht, R. E. Amaya, J. Shaker, and B. Syrett, "Side-lobe level reduction of half-mode substrate integrated waveguide leaky-wave antenna," *IEEE Trans. Antennas Propag.*, early access, Nov. 2020, doi: 10.1109/TAP.2020.3037806.
[49] N. Javanbakht, B. Syrett, and R. Amaya, "Leaky-wave antenna based on modified aperture half-mode substrate integrated waveguide," in *Proc. IEEE Int. Symp. Antennas Propag. USNC/URSI Nat. Radio Sci. Meeting*, Boston, MA, USA, Jul. 2018, pp. 1831–1832.
[50] Y. Dong and T. Itoh, "Composite right/left-handed substrate integrated waveguide and half mode substrate integrated waveguide leaky-wave structures," *IEEE Trans. Antennas Propag.*, vol. 59, no. 3, pp. 767–775, Mar. 2011.
[51] N. Javanbakht, M. S. Majedi, and A. R. Attari, "Thinned array inspired quasi-uniform leaky-wave antenna with low side-lobe level," *IEEE Antennas Wireless Propag. Lett.*, vol. 16, pp. 2992–2995, 2017.
[52] A. Mahmoodi Malekshah, M. S. Majedi, and A. R. Attari, "Improved design of a SIW long slot leaky wave antenna with low SLL," *IET Microw., Antennas Propag.*, vol. 13, no. 1, pp. 112–117, Jan. 2019.
[53] J. Liu, D. R. Jackson, Y. Li, C. Zhang, and Y. Long, "Investigations of SIW leaky-wave antenna for endfire-radiation with narrow beam and sidelobe suppression," *IEEE Trans. Antennas Propag.*, vol. 62, no. 9, pp. 4489–4497, Sep. 2014.
[54] Y. Mohtashami and J. Rashed-Mohassel, "A butterfly substrate integrated waveguide leaky-wave antenna," *IEEE Trans. Antennas Propag.*, vol. 62, no. 6, pp. 3384–3388, Jun. 2014.
[55] Q. Zhang, Q. Zhang, H. Liu, and C. H. Chan, "Dual-band and dual-polarized leaky-wave antenna based on slotted SIW," *IEEE Antennas Wireless Propag. Lett.*, vol. 18, no. 3, pp. 507–511, Mar. 2019.
[56] D. Zheng, Y.-L. Lyu, and K. Wu, "Longitudinally slotted SIW leaky-wave antenna for low cross-polarization millimeter-wave applications," *IEEE Trans. Antennas Propag.*, vol. 68, no. 2, pp. 656–664, Feb. 2020.
[57] Q. Lai, C. Fumeaux, W. Hong, and R. Vahldieck, "Characterization of the propagation properties of the half-mode substrate integrated waveguide," *IEEE Trans. Microw. Theory Techn.*, vol. 57, no. 8, pp. 1996–2004, Aug. 2009.
[58] N. Nguyen-Trong, T. Kaufmann, and C. Fumeaux, "A semi-analytical solution of a tapered half-mode substrate-integrated waveguide with application to rapid antenna optimization," *IEEE Trans. Antennas Propag.*, vol. 62, no. 6, pp. 3189–3200, Jun. 2014.
[59] M. Bozzi, A. Georgiadis, and K. Wu, "Review of substrate integrated waveguide circuits and antennas," *IET Microw., Antennas Propag.*, vol. 5, no. 8, pp. 909–920, 2011.
[60] D. M. Pozar, *Microwave Engineering*, 3rd ed. New York, NY, USA: Wiley, 2005.
[61] MACOM Technology Solutions. *MAVR-011020-14110 Datasheet (2nd ed.)* Accessed: Sep. 1, 2020. [Online]. Available: https://www.macom.com/products/product-detail/MAVR-011020-1411

NIMA JAVANBAKHT (Member, IEEE) received the B.Sc. and M.Sc. degrees in electrical engineering from the Ferdowsi University of Mashhad, Mashhad, Iran, in 2013 and 2016, respectively. He is currently pursuing the Ph.D. degree in electrical engineering with Carleton University, Ottawa, ON, Canada.

Since 2017, he has been a Research Assistant with the Department of Electronics, Carleton University. Furthermore, he has been a Research Intern with the National Research Council of Canada (NRC), since 2020. He has authored more than 20 technical papers in journals and conference proceedings. His research interests include the analysis and design of leaky-wave antennas, sidelobe suppression, reconfigurable antennas, compact microwave sensors, and 5G wireless networks.

Mr. Javanbakht's awards and honors include the Ontario Graduate Scholarship (OGS), the Doctoral Excellence Award, and CUASA Scholarship.

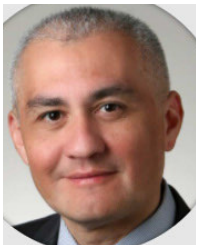

RONY E. AMAYA (Senior Member, IEEE) received the M.Eng. and Ph.D. degrees in electrical engineering from Carleton University, Ottawa, ON, Canada, in 2001 and 2005, respectively.

He joined the Design Center, Skyworks Solutions, Ottawa, in 2003, as a Senior Engineer, where he was involved in the design of RFIC for wireless transceivers. He also held the Research Scientist position with the Communications Research Centre, Canada, from 2006 to 2015, where he was involved in developing integrated RF circuit and system solutions from S-band to E-band and addressing packaging integration. He is currently an Associate Professor with the Department of Electronics, Carleton University. He has authored or coauthored more than 60 technical papers in journals and conference proceedings and holds several patents. His research interests include intelligent wireless communications systems making use of enabling microwave/RF technologies, such as smart engineered surfaces, gallium nitride and metamaterials, wireless power transfer, contactless communication links and power harvesting with applications to RFID and IoT systems, monolithic integrated Si/GaN/GaAs circuits, high-performance microwave circuit packaging, integrated active antennas, low temperature co-fired ceramics, and micro-electro-mechanical systems.

Dr. Amaya is also a member of the Association of Professional Engineers of Ontario.

JAFAR SHAKER (Senior Member, IEEE) received the B.Sc. degree in electrical engineering from the Iran University of Science and Technology, Tehran, Iran, in 1987, and the Ph.D. degree from the University of Manitoba, Winnipeg, MB, Canada, in 1995.

He has been a Research Scientist with the Communications Research Center, Ottawa, ON, Canada, since 1996. He is currently an Adjunct Professor with Carleton University, Ottawa, and the Royal Military College of Canada, Kingston, ON. He has authored or coauthored more than 50 technical papers in journals and conference proceedings. His current research interests include periodic structures, reflectarray, frequency selective surfaces (FSS), quasi-optical techniques, electronic band-gap structures, leaky-wave antennas, and the application of optical concepts in microwave and antenna engineering.

Dr. Shaker is also a member of the Association of Professional Engineers of Ontario.

BARRY SYRETT (Member, IEEE) received the B.Eng. and M.Eng. degrees in electrical engineering from Carleton University, Ottawa, ON, Canada, in 1971 and 1973, respectively, and the Ph.D. degree in electrical engineering from the University of Alberta, Edmonton, AB, Canada in 1976.

In 1976, he joined the Applied Instrumentation Laboratory, Department of Electronics, Carleton University, as a Senior Research Engineer, where he was involved in developing prototype electronic instrumentation systems. He was a Senior Industrial Fellow with Bell-Northern Research, Ottawa, in 1983 and 1991, where he was involved in the development of microwave radio systems. He was the Guest Scientist with the Institute for Information Technology, National Research Council, Ottawa, in 1991, where he was involved in optical interconnects and the Institute for Microstructural Sciences, National Research Council, Ottawa, 2001, where he was involved in photonic switches. Since 1977, he has been with the Department of Electronics, Carleton University, where he is currently a Professor of electrical engineering. He holds two patents in the area of microwave circuits. His current research interests include optoelectronic devices, monolithic microwave integrated circuits, photonic control of microwave circuits, and RF/microwave applications of metamaterials.

Dr. Syrett is also a Registered Professional Engineer in the province of Ontario, Canada.